2012

Decorin Expression, Straw-Like Structure, and Differentiation of Human Costal Cartilage

Michael W. Stacey
Old Dominion University, mstacey@odu.edu

Janna Grubb
Old Dominion University

Anthony Asmar
Old Dominion University

Julie Pryor
Old Dominion University

Hani Elsayed-Ali
Old Dominion University

See next page for additional authors

Decorin Expression, Straw-like Structure, and Differentiation of Human Costal Cartilage.

Journal:	*Connective Tissue Research*
Manuscript ID:	GCTS-2012-0023.R1
Manuscript Type:	Original Research
Date Submitted by the Author:	n/a
Complete List of Authors:	Stacey, Michael; Old Dominion University, Frank Reidy Research Center for Bioelectrics Grubb, Janna; Old Dominion University, Frank Reidy Research Center for Bioelectrics Asmar, Anthony; Old Dominion University, Frank Reidy Research Center for Bioelectrics Pryor, Julie; Old Dominion University, Frank Reidy Research Center for Bioelectrics Elsayed-Ali, Hani; Applied Research Center, Cao, Wei; Applied Research Center, Beskok, Ali; Old Dominion University, Institute of Micro and Nanotechnology Dutta, Diganta; Old Dominion University, Institute of Micro & Nanotechnology Fecteau, Annie; Hospital for Sick Children, Surgery Werner, Alice; Children's Hospital of the King's Daughters, Pediatric Pathology Darby, Dennis; Old Dominion University, Oceanography and Earth Sciences Kelly, Robert; Children's Hospital of the King's Daughters, Pediatric Surgery
Keywords:	pectus carinatum, chest wall deformity, SLRPs, AFM, gene ratio, connective tissue

Decorin Expression, Straw-like Structure, and Differentiation of Human Costal Cartilage.

Stacey MW[1,2], Grubb J[1], Asmar A[1], Pryor J[1], El-Sayed Ali[3] H, Cao W[3], Beskok A[4], Dutta D[4], Darby DA[5], Fecteau A[6], Werner A[7], Kelly RE Jr[8].

[1]Frank Reidy Research Center for Bioelectrics, Old Dominion University, Norfolk, VA USA

[2] Department of Pediatrics, Eastern Virginia Medical School, Norfolk VA USA

[3] Applied Research Center, Electrical and Computer Engineering, Old Dominion University, Norfolk, VA

[4]Institute of Micro & Nanotechnology, Old Dominion University, Norfolk, VA

[5] Oceanography and Earth Sciences, Old Dominion University, Norfolk, VA

[6] Division of General Surgery, Hospital for Sick Children, Toronto, Canada.

[7] Dept of Pathology, Eastern Virginia Medical School and Med Director of Laboratories, Children's Hospital of The King's Daughters, Norfolk VA

[8] Department of Surgery, Eastern Virginia Medical School and Pediatric Surgery Division, Children's Hospital of the King's Daughters, Norfolk VA

Corresponding author:
Dr. Michael Stacey, Frank Reidy Research Center for Bioelectrics, 4211 Monarch Way, Suite 300, Norfolk, VA 23508 USA
Email: mstacey@odu.edu
Telephone: 757 683 2245
Fax: 757 451 1010

Running head Human costal cartilage

Key Words Pectus carinatum, chest wall deformities, connective tissue, SLRPs, AFM, gene ratio,

ABSTRACT

Costal cartilage is much understudied compared to the load bearing cartilages. Abnormally grown costal cartilages are associated with the inherited chest wall deformities pectus excavatum and pectus carinatum resulting in sunken or pigeon chest respectively. A lack of understanding of the ultrastructural and molecular biology of costal cartilage is a major confounder in predicting causes and outcomes of these disorders. The present study analyzed the structure of marginal human costal cartilage (ribs 6-10) through scanning electron and atomic force microscopy and identified the presence of straw-like structures running longitudinally. We also demonstrated that chondrocytes tend to occur singly or as doublets and that centrally located cells produce high levels of aggrecan compared to more peripherally located cells measured by immunohistochemistry. Gene expression from mRNA extracted from cartilage showed high levels of decorin expression, likely associated with the large, complex tubular structures running through this cartilage type. *COL2A1, ACAN* and *TIMP1* also showed higher levels of expression compared to *ACTB*. Analysis of gene expression ratios demonstrate that costal cartilage is under differentiated compared to published ratios for articular cartilage, likely due to the vastly different biomechanical environments of each cartilage type. Further studies need to establish whether findings described here from the costal margins are significantly different to cartilage of the 'true ribs' and how these values change with age.

INTRODUCTION

Costal cartilage, a type of hyaline cartilage, connects each of ribs 1-5 to the sternum and ribs 6-10, which are fused, to the sternum as the costal margin. They remain cartilaginous throughout life and provide both strength and flexibility to the chest wall. Disorders of the chest wall can cause significant disfigurement with associated cardiac, pulmonary, and psychological manifestations and are classified as sunken chest (pectus excavatum, PE) or pigeon chest (pectus carinatum, PC) [1]. The costal cartilages of these patients are described as abnormally grown and weak. Disorders of costal cartilage are common, affecting approximately 1/400-1/1,000 individuals, show complex inheritance patterns in families, and affect primarily males (M4:F1) [2, 3, 4, 5]. Chest wall deformities are phenotypically variable and surgical repair outcomes can be unpredictable. The basic molecular characteristics that define a healthy human costal cartilage are largely unknown, and a lack of understanding of the ultrastructural and molecular biology of costal cartilage is a major confounder in predicting outcomes and causes chest wall deformities.

Recent work [6] described a decrease in the biomechanical stability of costal cartilage in pectus excavatum patients and suggested a disorderly arrangement and distribution of collagen fibers. Other authors have suggested that atypical collagen fibers may be implicated in chest wall deformities [7, 8]. The arrangement of collagen fibers in costal cartilage has not been described in detail; however, highly ordered fiber formation was described [9] in the surrounding perichondrium. Growth of human costal cartilage chondrocytes *in vitro* shows high levels of *COL2A1* and *ACAN* expression and low levels of *COL1A1* at low culture passage, typical of a differentiated cell [10]. Differences in the variable number of tandem repeat units of chondroitin sulphate attachment sites were observed in *ACAN* with significantly more repeats (27) being present in patients with chest wall deformities [11].

TGFβ1 signaling plays a key role in cartilage growth and ECM turnover. Cells are extremely sensitive to levels of TGFβ1 and, therefore, regulation of this growth factor is important in normal growth and development. Genes activated via TGFβ pathways include *SOX9*, a major transcription factor of chondrocyte differentiation and regulator of

ACAN and *COL2A1* expression. In addition, *TIMP1,* a regulator of the matrix metalloproteinase's (MMP 8 and 13), is positively regulated by the TGFβ1 pathway [12].

Small leucine-rich proteoglycans (SLRPs) are small proteoglycans that are highly expressed in cartilage. Regulation of collagen fibrillogenesis is an important function shared by many SLRPs, and null mutations have been shown to lead to abnormal collagen architecture in mice [13]. Additionally, SLRPs mediate cell metabolism by binding to growth factors, including members of the superfamily TGFβ1 [14]. The causes of PE and PC are unknown; however, SLRPs can regulate ECM growth and fibrillogenesis by controlling TGFβ availability, suggesting a mechanistic role for SLRPs in these disorders. Biglycan deficiency has been shown to cause spontaneous aortic dissection and rupture in mice [15], and is also a characteristic of Marfan syndrome, a syndrome known to exhibit chest wall deformities. Decorin function is consistent with functions related to fibrillogenesis [16, 17]. A critical concept of SLRP function is compensation of one SLRP function over another. In the absence of biglycan, decorin is up-regulated and, therefore, differences in gene expression ratios may be apparent. Our central hypothesis is that abnormal expression of *BGN* and *DCN* will be observed in patients with chest wall deformities.

A thorough knowledge on the expression patterns of genes responsible for chondrogenesis in costal cartilage would provide insights into the role of these proteins in chest wall deformities and offer a biological rationale for the variability observed in outcome of surgery [18, 19, 20]. The objective of this study was to identify ultrastructural morphology and protein localization, investigate relative levels of expression of key genes required for chondrogenesis, and compare changes in normal costal cartilage and chest wall deformity.

MATERIALS AND METHODS

2.1 Subjects

Human costal cartilage was obtained from 4 patients with pectus carinatum severe enough to warrant surgical repair. Informed consent was obtained following IRB approval of the protocol at Eastern Virginia Medical School. The IRB protocol currently prevents disclosure of many clinical features, and thus close correlation of clinical

phenotype with expression is not possible. Costal cartilage samples were collected from ribs 6-8 at surgery.. Experiments were performed on the round, rod-like, mid-sections of cartilage. All patients were male, with an age range of early teen to early 20's. Apparently normal costal cartilage was obtained from an age-matched-control, a 15 year old male and processed within 24 hours. All samples were snap frozen in liquid nitrogen and stored at -80^{o}C until use.

2.2 Ultrastructural analysis

Scanning electron microscopy (SEM) is a well-described technique employed for ultrastructural studies of cells and tissues. Cartilage, samples were cut into small sections approximately 3mm thick, washed three times in Sorenson's buffer and digested at 37^{o}C for 48 hours in trypsin (1mg/ml) and hyaluronidase (1mg/ml) in Sorenson's buffer [21]. Samples were washed thoroughly in PBS and fixed in 2.5% glutaraldehyde in phosphate buffered saline for 2.5 hours. Samples were rinsed in deionized water, dehydrated through an ethanol series, dried and mounted on carbon discs, gold sputtered, and examined using a JSM-6060LV SEM (JEOL, Tokyo, Japan) operating at 5 keV to minimize sample damage. Images were captured electronically and fiber measurements made using Image J software.

2.3 Atomic Force Microscopy (AFM)

Collagen straws were released from small pieces of tissue by brief homogenization and digestion with 0.1mg/ml hyaluronidase and 0.1mg/ml trypsin in Sorenson's buffer. Samples were fixed in ice cold acetone and fiber diameters measured using a Nanonics Multiview-4000 multi-probe AFM.

2.4 Immunohistochemistry

Confirmation of aggrecan gene expression and protein distribution were made by immunohistochemistry. Frozen cartilage samples were mounted in CRYO-OCT Compound (Tissue-Tek, CA USA) and sections (5µm) generated using a Microm HM525 cryostat. Sections were fixed in ice-cold acetone. Blocking, incubation with primary and secondary antibodies and washing were performed following manufacturer's guidelines for each antibody. Tissues were incubated with a mouse monoclonal antibody specific for aggrecan (sc-73693, Santa Cruz, Santa Cruz, CA). The antibody was raised against recombinant aggrecan from human origin Negative controls were produced using

normal mouse IgG included in the ImmunoCruz mouse LSAB staining system (sc-2050, Santa Cruz). Electronic images were captured using a CCD camera through an Olympus BX51 with Metamorph and Image J software for semi and quantitative analysis of protein deposition.

2.5 Chondrocyte distribution

Cartilage consists mainly of proteoglycans and collagens, with chondrocytes sparsely distributed throughout the matrix. We catalogued the distribution pattern of 586 and 999 chondrocytes in transverse sections of costal cartilage from PC3 and Con3 respectively, through an Olympus BX51 microscope, as groups of 1-4+ cells per cluster located interiorly or peripherally. Interior cells were within the strongly expressing aggrecan region, and peripheral cells outside.

2.6 Reverse Transcription and Real-Time PCR Analysis

Cartilage was removed from -80^{o}C and transverse sections cut at approximately 3-5mm on dry ice and placed into RNALater (Qiagen, CA USA). Samples were quickly weighed and approximately 100mg of costal cartilage was ground to a powder with a liquid nitrogen immersed pestle and mortar. RNA was isolated and genomic DNA eliminated by completing RNA extraction using a RNeasy Plus Mini Kit and RT-First Strand Kit (Qiagen, CA USA). All polymerase chain reactions (PCR) were performed on a BioRad CFX96 system in 25µl reactions using SYBR green detection (Qiagen, CA USA). Gene expression by PCR was performed on genes described in Table 1, all compared to the housekeeping gene *ACTB*. All primers were from Qiagen, CA USA. The reaction conditions were identical for all primers, 95^{o}C for 10 minutes, then 40 rounds of 95^{o}C for 15 seconds and 60^{o}C for 60 seconds. Reaction specificities were assessed with a melt curve of 65^{o}C to 95^{o}C in 0.2^{o}C increments. All experiments were in triplicate and performed with positive and negative controls. At least two independent extractions were included from samples stored at 4^{o}C in RNALater. Data were standardized to housekeeping *ACTB* values for all samples using the delta Ct method.

2.7 Statistical Analysis

Statistical analysis was performed using Student t-test to determine significance between sample and control means. For all tests, $p < 0.05$ indicated the difference as significant.

RESULTS

3.1. Electron Microscopy and AFM

Costal cartilage is a much understudied tissue type, both ultra structurally and genetically. We provide a first description of these properties in samples of human costal cartilage. Figures 1a and 1b are representative SEM images of a transverse cross-section of costal cartilage taken from a mid-section. Figure 1a shows a fracture in the cartilage, estimated as the inner-middle zone, exposing collagen fibers of approximately 600nm diameter. Fibers are assembled into extremely large complexes of many µm (arrowed) that run parallel to the length of the cartilage. Figure 1b is a higher magnification of the boxed area and shows that each fiber forms a nanostraw of approximately 650nm external diameter and 250nm internal lumen diameter. Images of longitudinal sections show a well-defined organization of collagen fibers approximately 20µm diameter and cellular lacunae (Figure 1c). We measured the diameters from 150 clearly defined fibers from SEM images (Table 2) and found that most were in the range from 0.1-100 µm. The smallest (<0.1µm) would most-likely represent the collagen fibrils, the midsize (~1µm) would represent the "microtubes" and the largest (~100µm) would be large fascicle-like structures. Cartilage homogenization and digestion released nanostraw fibers and allowed further characterization by AFM. Figure 1d shows an AFM image of branching/splitting fibers with a maximum diameter of approximately 740nm. Clearly, costal cartilage has large fiber dimensions with complex structures formed through finely tuned fibrillogenesis.

3.2 Aggrecan immunohistochemistry

Aggrecan deposition from cells appeared to be a function of location. Figure 2 shows a representative cross-section of costal cartilage with cells located centrally exhibiting intense aggrecan staining (A) compared to the more peripherally located cells (B) and outer most cells (C). Interestingly, we were able to show increased levels of sodium ions in the same central region by electron probe microanalysis (EPMA, supplemental figure), showing that positively charged ions were drawn in to achieve electroneutrality.

3.3 Chondrocyte distribution

The organization of chondrocytes in cartilage is not considered to be random, and different cartilage types have different configurations of singles, pairs, clusters or strings

of cells. The percentage number of cell clusters observed in the interior was 1 cell (68.5% and 60.2%), 2 cells (23% and 27.3%), 3 cells (4.3% and 10.1%) and 4+ cells (4.2% and 2.4%) respectively for PC3 and Control. For peripherally located cells, observed clusters were 1 cell (86.9% and 73.0%), 2 cells (12.6% and 19.7%), 3 cells (0.5% and 5.5%) and 4+ cells (0% and 1.8%) respectively for PC3 and Control. There is a trend towards higher cell clusters in the interior; however, there appears to be no differences in cell distribution between PC3 and age-matched control.. No strings were observed.

3.4 Gene expression

Due to the unusual structure of costal cartilage we undertook analysis of gene expression to determine presence of the main constituents of cartilage; collagen type II, and the large aggregating proteoglycan, aggrecan. We also examined other genes that play a role in growth, structure and differentiation of cartilage. *BGN, NYX, CACNA1F* and *TIMP1* were of interest because these genes are located on the human X-chromosome, where affected individuals are predominantly male and possess only a single X-chromosome [2, 3].

Costal cartilage from individuals with chest wall deformities is described as abnormally grown and weak. Typically, surgical repair takes place during teenage years to early 20's. Phenotypically, there is considerable variation of the clinical condition of PC, reflecting the complex nature and inheritance observed in these families. Variation in gene expression between samples is, therefore, expected; however, it is unknown whether the expression of matrix genes will be affected by surgical procedures. We compared gene expression of 4 patients with pectus carinatum to an age-matched-control. Table 3 shows *COL2A1*, *DCN, ACAN,* and *TIMP1* are all highly expressed compared to *ACTB*. Sample variation was noted, although, as expected, *COL2A1* was expressed to the highest level in all samples.

Compared to control, PC1 showed significant reduction in expression of *DCN* ($p<0.001$) and *TIMP1* ($p<0.001$). PC3 showed significantly lower expression of *COL2A1* ($p<0.001$) and like PC4, both showed decreased expression of *ACAN* ($p<0.03$ and $p<0.024$, respectively). PC4 also showed significantly higher expression of *TIMP1* ($p<0.001$) and decreased expression of *BGN* ($p<0.04$). PC2 showed significant reduction in expression of *COL2A1* ($p<0.01$), *DCN* ($p<0.0002$), *TIMP1* ($p<0.001$), *BGN* ($p<0.03$)

and *FBN1* ($p<0.01$). This sample, like all PC samples, was immediately processed from the operating room, although results suggest possible degradation of this sample.

Many patients with chest wall deformities are considered Marfanoid-like [22] without fulfilling all criteria for diagnosis of Marfan syndrome, including mutations of the fibrillin-1 gene. The expression of this gene was not significantly different between control and patients, with the exception of PC2 ($p<0.01$). Expression of the X-linked genes *NYX* and *CACNA1F* was not detected in any samples. Overall, deregulation of *TIMP1* expression was evident in 3/4 PC samples, and expression of *DCN* was significantly lower in 2/4, suggestive of roles for fibrillogenesis and matrix turnover. The differentiation status of cartilage can be equated to the ratio of *COL2A1*, present in differentiated cartilage, to *COL1A1*, present at higher levels in more undifferentiated cartilage. We compared ratios of gene expression to published data. Ratios of the differentiation markers *COL2A1:ACAN* and *COL2A1:COL1A1* are low in PC patients and control (Table 4) compared to rabbit articular cartilage (1090 and 1790, respectively) but both are highly comparable to the nucleus pulposus region of lumbar discs (23 and 930 respectively), [23]. The ratios of *ACAN:COL1A1* fall between those reported for fully differentiated rat chondrosarcoma cells (78.4) and dedifferentiated chondrocytes cultured from costal cartilage (4.6) [24]. A high expression ratio of *COL2A1:COL1A1* (294.6) in human articular cartilage has been reported [25], but here results are referenced to *GAPDH* rather than *ACTB*. Overall, these results suggest costal cartilage is at an intermediate stage of differentiation and likely represents the different functional requirements of this tissue compared to articular cartilage. Small differences exist between patients and between patients and control (Table 4), suggesting that gene ratios measured here are not major contributors to chest wall abnormalities in these samples. Interestingly, *DCN* is expressed at high levels compared to *BGN*. As well as binding growth factors, both SLRPs have a role in fibrillogenesis and were hypothesized to play a role in the etiology of chest wall deformities. The high *DCN/BGN* ratio strongly suggests the importance of decorin expression in costal cartilage morphology. Decorin is present at high levels during tendon (fibro-cartilage) development and persists until thick fibers are formed [26], thus parallels with costal cartilage (hyaline cartilage) are apparent.

DISCUSSION

Costal cartilage is a much understudied cartilage where deformities have significant clinical consequences. A lack of understanding of molecular and ultrastructural properties hampers understanding events leading to these disorders. The present study compared relative gene expression of major genes of chondrogenesis from patients with pectus carinatum to an age-matched-control to answer questions relating to maintenance and differentiation. Perhaps the most important observations are 1) the longitudinal straw-like arrangement of collagen fibers, 2) the centrally located deposition of aggrecan, 3) the high level of decorin expression, and 4) gene ratios indicating under differentiation compared to articular cartilage.

The ultrastructural electron microscopy images show that human costal cartilage is unlike other cartilage types. Images appear to show that individual fibers are assembled to collectively form very thick, fascicle structures appearing to consist of large numbers of collagen nanostraws that run parallel along the cartilage length. A similar observation of collagen tubules in juvenile rabbit tibia articular cartilage was reported [27], but this is the first report in human costal cartilage. The cartilage template of long bones is similar to costal cartilage in that they are both long, thick, rod-like structures and, therefore, although functionally different, ultrastructural similarities may be expected in response to cell maintenance and collagen fiber deposition under these conditions.

The morphological form of costal cartilage and how this relates to function is currently unknown. The presence of straw-like structures may provide strength and a means of gas and nutrient exchange to cells by fluid flow whose movement is dependent upon cartilage movement during breathing. Costal cartilage can be nearly 1cm diameter, outside of the range of diffusion to maintain centrally located cells [28]. Hypoxia or low pH has been shown to act as a trigger for aggrecan and collagen type II production through induction of hypoxia inducible factor 1-α and *SOX9*, as well as inhibit *COL1A1* expression [29, 30]. Similarities with inter vertebral discs are noteworthy. Cells embedded within the centrally located nucleosus pulposus experience hypoxia and express aggrecan under the regulation of the hypoxia induced P13K/AKT signaling pathways via modulation of *SOX9* [31]. It appears that as cells become centrally located

they experience hypoxia and lower pH. *ACAN* expression is induced with cationic uptake that we confirmed by Electron Probe Micro Analysis.

Few studies have been undertaken on chondrocyte distribution within cartilage, yet cell density and arrangements are considered to be critical to function. Cellular clusters [32], pairs [33], and rows [34], have been reported. A more extensive study [35] in the superficial zone of articular cartilage identified complex patterns that appear to be location specific. A spatial relationship between collagen fiber alignment and cellular organization was suggested [34], with chondrocytes running parallel to adjacent fibers. Longitudinally, we also note the presence of lacunae between the large fibrous structures. The predominance of single and doublets in costal cartilage suggests cells undergo relatively few divisions. The absence of extensive strings and clusters is likely due to the different biomechanical forces experienced by costal cartilage compared to cartilage covering ball and socket joints.

SLRPs play an important role in fibrillogenesis and shape the architecture and mechanical properties of the collagen matrix. SLRP-deficient animals exhibit a wide array of diseases, mostly resulting from abnormal fibrillogenesis [13]. We examined the expression of three SLRPs; *DCN* and the X-linked genes *BGN* and *NYX*. *NYX* expression was not detected in any samples of costal cartilage and likely does not play a role in chondrogenesis. *DCN* has a role in modulating cartilage fibril growth, thickness, and orientation. Indeed, *DCN* deficiency introduces tissue-specific variations in range, mean, and distribution of collagen fibril diameters compared to wild-type. Interestingly, *DCN* deficiency also leads to random orientation of collagen fibrils in periodontal ligament instead of the usual parallel orientation [36]. Regional variation in localization of proteoglycans decorin, biglycan, and aggrecan has been reported in tendon, with decorin highest in regions of greatest tensile strength [37]. However, tensile strength of costal cartilage appears to reduce as it matures from childhood to teenage/early twenties years [38], suggesting rearrangement of collagen fibers with age that may be proteoglycan mediated. The highly aligned collagen fibers observed in costal cartilage show similarities to the aligned fibers of tendon. The hierarchical assembly of collagen fibers in tendon is a multistep process leading to the mature tissue [39]. Briefly, collagen fibril intermediates are assembled and undergo linear and lateral growth. Intercalation of fibrils

is necessary for growth resulting in mature fibers and fibrils necessary for mechanical integrity. The interactions with fibril associated collagens and SLRPs have been implicated in the form and function of mature tendon. In costal cartilage an additional layer of complexity in the formation of tubules is intriguing, and suggests, by the high level of *DCN* expression, that decorin is crucial in this morphology.

The relative expression of genes expressed as a ratio has been used to determine differentiation status of cartilage where *COL2A1* and *ACAN* are highly expressed compared to *COL1A1*. This ratio decreases rapidly as chondrocytes dedifferentiate *in vitro*. Adaption of tissue to its mechanical constraints leads to different qualitative compositions. Costal cartilage exhibits a phenotype consistent with cartilage, with high *COL2A1/COL1A1, COL2A1/ACAN* and *ACAN/COL1A1*ratios, although *COL2A1/ACAN* and *COL2A1/COL1A1*ratios were considerably lower than rabbit articular cartilage also normalized to *ACTB* [24] suggesting *COL2A1* expression may be reduced. Expression levels in costal cartilage are closer to those reported in the nucleus pulposus of lumbar discs than to articular cartilage. Both nucleus pulposus and costal cartilage expression levels likely represent the functional requirements of their respective mechanical loads that are considerably different to that experienced in articular cartilage.

The present study has uncovered a new dimension of complexity that has not previously been reported. The study here describes findings that are generated from samples of costal cartilage that are generally removed at surgery, ribs 6-8. Although the current study has relatively few samples we feel that the overall results indicate that there are several important features unique to costal cartilage. Future work will examine variations along and between different ribs to more closely correlate variations of functions that may occur within the environment of the chest wall. Connective tissue gene arrays will allow analysis of many more genes simultaneously correlated to clinical picture. The etiology of chest wall deformity is complex. Changed growth characteristics of costal cartilage in patients may be a secondary characteristic due to external factors. Alternatively deformed cartilage may be intrinsic due to the inherited, albeit complex, nature of these disorders. Future work will aim to clarify these discrepancies.

Acknowledgments

We thank Dr M. Young, National Institute of Dental and Craniofacial Research, NIH and Dr C. Osgood, College of Sciences, Old Dominion University for critical review of this manuscript, and Old Dominion University Office of Research for seed funding grant.

Declaration of interest: The authors have declared no conflict of interest.

References

[1] Kelly RE, Shamberger RC, Mellins RB, Mitchell KK, Lawson ML, Oldham K, Azizkhan RG, Hebra AV, Nuss D, Goretsky MJ, Sharp RJ, Holcomb GW, Shim WKT, Megison SM, Moss RL, Fecteau AH, Colombani PM, Bagley TC and Moskowitz AB. Prospective Multicenter Study of Surgical Correction of Pectus Excavatum: Design, Perioperative Complications, Pain, and Baseline Pulmonary Function Facilitated by Internet-Based Data Collection. J.Am. College of Surgeons. (2007) 205: 205-216

[2] Horth L, Stacey MW, Benjamin T, Segna K, Proud VK, Nuss D, Kelly RE. Genetic analysis of inheritance of *Pectus excavatum.* J. Pediatric Genetics. (2012) In press

[3] Creswick H, Stacey M, Kelly R, Burke B, Gustin T, Mitchell K, Nuss D, Harvey H, Croitoru D, Goretsky M, Vasser E, Fox P, Goldblatt S, Tabangin M, Proud V. Family studies on the inheritance of pectus excavatum. J. Pediatr. Surg. (2006) 41:1699-1703

[4] Leung AK, Hoo JJ. Familial congenital funnel chest. Am. J. Med. Genet. (1987). 26: 887-890

[5] Sugiura, Y. A family with funnel chest in three generations. Jpn. J. Hum. Genet. (1977). 22: 287-289.

[6] Feng J, Hu T, Liu W, Zhang S, Tang Y, Chen R, Jiang X, Wei F. The biomechanical, morphologic, and histochemical properties of the costal cartilages in children with pectus excavatum. J. Pediat. Surg. (2001). 36: 1770-1776.

[7] Rupprecht H, Hümmer, HP. Stöß, H. Waldherr T. Pathogenesis of the Chest Wall Deformities - Electron Microscope Studies and Analysis of Trace Elements in the Cartilage of the Ribs. Eur J Pediatr Surg (1987). 42(4): 228-229

[8] Fokin AA, Nury M. Steuerwald M, Ahrens William A, Allen KE. Anatomical, Histologic, and Genetic Characteristics of Congenital Chest Wall Deformities. Semin Thorac Cardiovasc Surg. (2009). 21(1):44-57

[9] Forman JL, del Pozo de Dios E, Dalmases CA, Kent RW. The contribution of the perichondrium to the structural mechanical behavior of the costal-cartilage. J. Biomech. Eng. (2010) 132; /094501 doi: 10.1115/1.4001976

[10] Zhang Y, Chai G, Liu W, Cui L,Cao YL. Age-related changes in growth and metabolism function of human costal chondrocytes cultured in vitro. Zhonghua Zheng Xing Wai Ke Zhi (2004) 20; 372-376

[11] Stacey M, Neumann S, Dooley A, Segna K, Kelly R, Nuss D, Kuhn A, Goretsky M, Fecteau A, Pastor A, Proud V. Variable Number of Tandem Repeat Polymorphisms (VNTRs) in the *ACAN* Gene Associated with Pectus Excavatum. Clin. Genet. (2010). 78;502-504

[12] El Mabrouk M, Qureshi HY, Li QW, Sylvester J, Zafarullah M. Interleukin-4 antagonizes oncostatin M and transforming growth factor beta-induced responses in articular cartilage. J. Cell. Biochem. (2008).103: 588-597.

[13] Ameye L, Young MF. Mice deficient in small leucine-rich proteoglycans: novel in vivo models for osteoporosis, osteoarthritis, Ehlers-Danlos syndrome, muscular dystrophy, and corneal diseases. Glycobiology (2002).12: 107R-116R.

[14] Hildebrand A, Romaris M, Ramussen LM, Heingard D, Twardzik DR, Border WA, Ruoslahti E Interaction of the small interstitial proteoglycans biglycan, decorin and fibromodulin with transforming growth factor β. Biochem. J. (1994). 302: 527-534

[15] Heegaard AM, Corsi A, Danielsen CC, Nielsen KL, Jorgensen HL, Riminucci M, Young MF, Bianco P. Biglycan Deficiency Causes Spontaneous Aortic Dissection and Rupture in Mice. Circulation. (2007);115:2731-2738.

[16] Bianco P, Fisher LW, Young MF, Termine JD, Robey PG. Expression and localization of the two small proteoglycans biglycan and decorin in developing human skeletal and non-skeletal tissues. J. Histochem. Cytochem. (1990). 38: 1549-1563

[17] Kalamajski S, Oldberg A. The role of small leucine-rich proteoglycans in collagen fibrillogenesis. Matrix Biol. (2010) 29; 248-253

[18] Antonoff MB, Saltzman DA, Hess DJ, Acton RD. Retrospective review of reoperative pectus excavatum repairs. J. Pediatr Surg. (2010). 45(1):200-5.

[19] Bouchard S, Hong AR, Gilchrist BF, Kuenzler KA. Catastrophic cardiac injuries encountered during the minimally invasive repair of pectus excavatum. Semin. Pediatr. Surg. (2009) 18(2):66-72.

[20] Swanson JW, Colombani PM. Reactive pectus carinatum in patients treated for pectus excavatum. J. Pediatr. Surg. (2008). 43(8):1468-73.

[21] Stolz M, Gottardi R, Raiteri R, Miot S, Martin I, Imer R, Staufer U, Raducanu A, Düggelin M, Baschong W, Daniels AU, Friederich NF, Aszodi A & Aebi U. Early detection of aging cartilage and osteoarthritis in mice and patient samples using atomic force microscopy. Nature Nanotechnology (2009) 4; 186-192

[22] Redlinger RE Jr., Rushing GD, Moskowitz AD, Kelly RE, Jr., Nuss D, Kuhn A, Obermeyer RJ, Goretsky MJ. Minimally invasive repair of pectus excavatum in patients with Marfan Syndrome and Marfanoid features. J. Pediatr. Surg. (2010). 45(1): 193-199

[23] Clouet J, Grimandi G, Pot-Vaucel M, Masson M, Fellah HB, Guigand L, Cherel Y, Bord E, Rannou F,Weiss P, Guicheux J and Vinatier C. (2009). Identification of phenotypic discriminating markers for intervertebral disc cells and articular chondrocytes. Rheumatology (2009) 48 (11): 1447-1450.

[24] McAlinden A, Havlioglu N, Liang L, Davies SR, Sandell LJ. Alternative Splicing of Type II Procollagen Exon 2 Is Regulated by the Combination of a Weak 5′ Splice Site and an Adjacent Intronic Stem-loop Cis Element. J. Biol. Chem. (2005). 280; 32700-32711

[25] Martin I, Jakob M, Schafer D, Dick W, Spagnoli G, Heberer M. Quantitative analysis of gene expression in human articular cartilage from normal and osteoarthritic joints. Osteoarthr. Cartilage (2001) 9; 112-118

[26] Kalamajski S, Oldberg A. The role of small leucine-rich proteoglycans in collagen fibrillogenesis. Matrix Biology (2010) 29; 248-253

[27] Gwynn AP, Wade S, Kääb MJ, Owen GR, Richards RG. Freeze-substitution of rabbit tibial articular cartilage reveals that radial zone collagen fibers are tubules. J. Microsc. (2000) 197; 159-172

[28] Gibson JS, Milner PI, White R, Fairfax TP, Wilkins RJ. Oxygen and reactive oxygen species in articular cartilage: modulators of ionic homeostasis. Pflugers Arch. (2008) 455; 563-573

[29] Duval E, Leclercq S, Elissalde JM, Demoor M, Galera P, Boumediene K. Hypoxia-inducible factor 1α inhibits the fibroblast-like markers type I and type III collagen during hypoxia-induced chondrocyte redifferentiation. Arthritis Rheum. (2009) 60; 3038-3048

[30] Das RHJ, van Osch GJVM, Kreukniet M, Oostra J, Weinans H, Jahr H Effects of individual control of pH and hypoxia in chondrocyte culture. J. Orthop. Res. (2010). 28; 537-545

[31] Chin-Chang Cheng, Yoshiyasu Uchiyama, Akihiko Hiyama, Sachin Gajghate, Irving M. Shapiro, and Makarand V. Risbud. PI3K/AKT Regulates Aggrecan Gene Expression by Modulating Sox9 Expression and Activity in Nucleus Pulposus Cells of the Intervertebral Disc. J. Cell Physiol (2009) 221; 668-676

[32] Schumacher BL, Su JL, Lindley KM, Kuettner KE, Cole AA. Horizontally oriented clusters of multiple chondrons in the superficial zone of ankle, but not knee articular cartilage. Anat. Rec. (2002). 266; 241-248

[33] Jadin KD, Wong BL, Bae WC, Li KW, Williamson AK, Schumacher BL, Price JH, Sah RL. Depth-varying density and organization of chondrocytes in immature and mature bovine articular cartilage assessed by 3d imaging and analysis. J. Histochem. Cytochem. (2005). 53; 1109-1119

[34] Clark JM, Rudd E. Cell patterns in the surface of rabbit articular cartilage revealed by the backscatter mode of scanning electron microscopy. J. Orthop. Res. (1991). 9; 275-283

[35] Rolauffs B, Williams JM, Grodinsky AJ, Kuettner KE, Cole AA. Distinct horizontal patterns in the spatial organization of superficial zone chondrocytes of human joints. J. Struct. Biol. (2008). 162; 335-344

[36] Hakkinen L, Strassburger S, Kahari VM, Scott PG, Eichstetter I, Lozzo RV, Larjava H. A role for decorin in the structural organization of periodontal ligament. Lab. Invest. (2000) 80; 1869-1880

[37] Matuszewski PE, Chen YL, Szczesny SE, Lake S, Elliot DM, Soslowsky LJ, Dodge GR. Regional variation in human supraspinatus tendon proteoglycans: decorin, biglycan, and aggrecan. Connect. Tissue Res. (2012). Jan 6 Epub ahead of print.

[38] Yang Qing-Hua, Song Yu-Peng, Jiang Haiyue, Zhuang Hong-Xing. The significance of the biomechanical properties of costal cartilage in the timing of ear reconstruction surgery. J. of Plastic, Reconstructive and Aesthetic surgery (2011). 64; 742-746

[39] Zhang G, Young BB, Ezura Y, Favata M, Soslowsky, Chakravarti S, Birk DE. Development of tendon structure and function: Regulation of collagen fibrillogenesis J. Musculoskelet Neuronal Interact. (2005) 5; 5-21

TABLES

Table 1. A description of genes investigated in this study.

Gene	Name	Chromosome Location	Description
ACTB	β-Actin	7p22	Housekeeping
ACAN	Aggrecan	15q26.1	Large aggregating proteoglycan
BGN	Biglycan	Xq28	Small proteoglycan (SLRP)
CACNA1F	Voltage-gated calcium channel-α1F	Xp11.23	Voltage-sensitive calcium channel
CAL1A1	Collagen α-1 chain	17q21.33	Type I collagen fiber
CAL2A1	Collagen type II α-1	12q13.11	Type II collagen fiber
DCN	Decorin	12q21.33	Small proteoglycan (SLRP)
FBN1	Fibrillin 1	15q21.1	Large extracellular matrix glycoprotein
NYX	Nyctalopin	Xp11.4	Small proteoglycan (SLRP)
SOX9	SRY (Sex determining region Y)-box 9	17q24.3	Transcription regulator
TGFβ1	Transforming Growth Factor-β1	19q13.2	Growth factor
TIMP1	Tissue inhibitor of metalloproteinase 1	Xp11.23	Inhibitor of matrix metalloproteinases

Table 2. Distribution of collagen fiber diameters in costal cartilage measured from SEM images.

Fiber Dia.	0-0.09µm	0.1-0.99µm	1-9.9 µm	10-100 µm
% of total	14.9	34	8.5	42.6
Median	0.08	0.426	1.036	21.5
Range	0.043-0.089	0.113-0.898	1.01-1.055	12.36-95.2

Table 3. Fold difference in gene expression (+/- SE) of four patients with pectus carinatum and an age-matched control compared to β-actin. Significant differences in expression between control and patients are marked with *

	Control	PC1	PC2	PC3	PC4
COL2A1	134.0+/-7.06	134.31+/-49.33	*84.09+/-10.42	*46.96+/-12.22	118.79+/-10.24
ACAN	3.12+/-0.69	3.79+/-1.4	2.89+/-0.26	*1.30+/-0.15	*6.38+/-0.989
DCN	17.63+/-2.25	*4.47+/-0.51	*4.31+/-0.71	16.21+/-0.71	20.58+/-2.18
TIMP1	3.18+/-0.47	*0.67+/-0.07	*0.91+/-0.159	3.39+/-0.01	*5.53+/-0.46
ACTB	1	1	1	1	1
BGN	1.39+/-0.49	0.59+/-0.07	*0.33+/-0.09	0.84+/-0.01	*0.3+/-0.054
COL1A1	0.12+/-0.03	0.15+/-0.03	0.12+/-0.02	0.11+/-0.04	0.12+/-0.02
FBN1	0.46+/-0.08	NA	*0.18+/-0.01	0.49+/-0.05	0.30+/-0.15
SOX9	0.33+/-0.10	0.30+/-0.17	0.20+/-0.02	0.15+/-0.001	0.63+/-0.098
TGF-β1	0.18+/-0.09	0.15+/-0.021	0.13+/-0.041	0.09+/-0.016	0.04+/-0.005

Table 4. Gene expression ratios in costal cartilage from pectus carinatum and control.
Published values are for cells of the lumbar nucleus pulposus (NP) and annulus fibrosus (AF) regions, and articular cartilage (AC), with references [ ].

	COL2A1/ACAN	***COL2A1/COL1A1***	***ACAN/COL1A1***	***DCN/BGN***
PC1	35.44	877.80	24.77	7.58
PC2	29.10	700.75	24.08	13.06
PC3	36.12	426.91	11.82	19.34
PC4	18.62	989.92	53.17	69.06
Control	42.95	1116.7	26	12.68
Published	23 NP [23] 370 AF [23] 1090 AC [23]	930 NP [23] 26 AF [23] 1790 AC [23]	4.6 *in vitro* [24] 78.4 sarcoma [24]	

Figure Legends

Figure 1. SEM and AFM images of normal costal cartilage. A. Transverse section (x2500) showing large numbers of dense fibrils running longitudinally (arrowed). B. Magnification (x10,000) of the boxed area in A and shows the presence of collagen nanostraws (arrowed). Each straw is approximately 650nm in diameter. C. Longitudinal section (x500) showing bundles of collagen fibers, formed from multiple collagen nanostraws, of approximately 20µm diameter (white arrow). D. Atomic force microscopy image of isolated collagen nanostraws of approximately 740nm maximal diameter (arrowed).

Figure 2. Localization of aggrecan by immunohistochemistry in transverse cross-sections of costal cartilage. A: Distribution of aggrecan in whole control section. B: Distribution of aggrecan in whole PC3 section. C-E: Distribution of aggrecan in control at 10x magnification from (C) periphery, (D) midzone, and (E) interior regions. Scale bars, 100 µm. F-H: Distribution of aggrecan of aggrecan in control at 100x magnification from (F) periphery, (G) midzone, and (H) interior regions. Scale bars, 10 µm. Notice the localization of aggrecan becomes more intense around each lacuna in the interior compared to the periphery.

1a

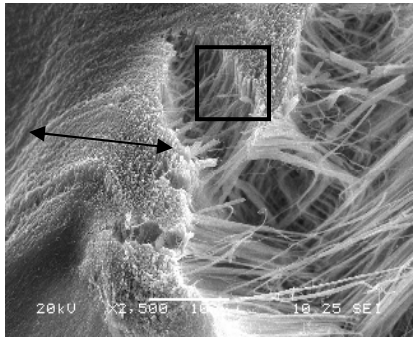

1b

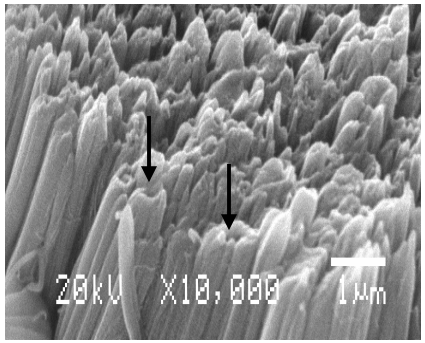

1c

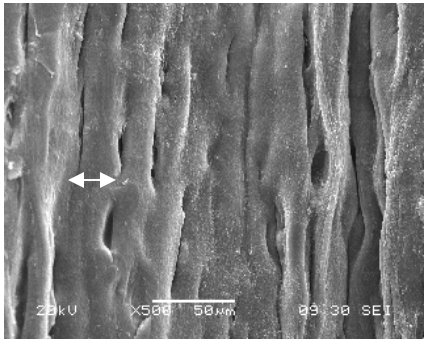

1d

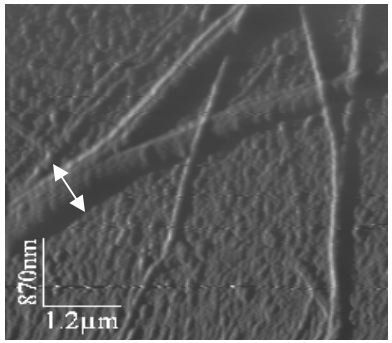

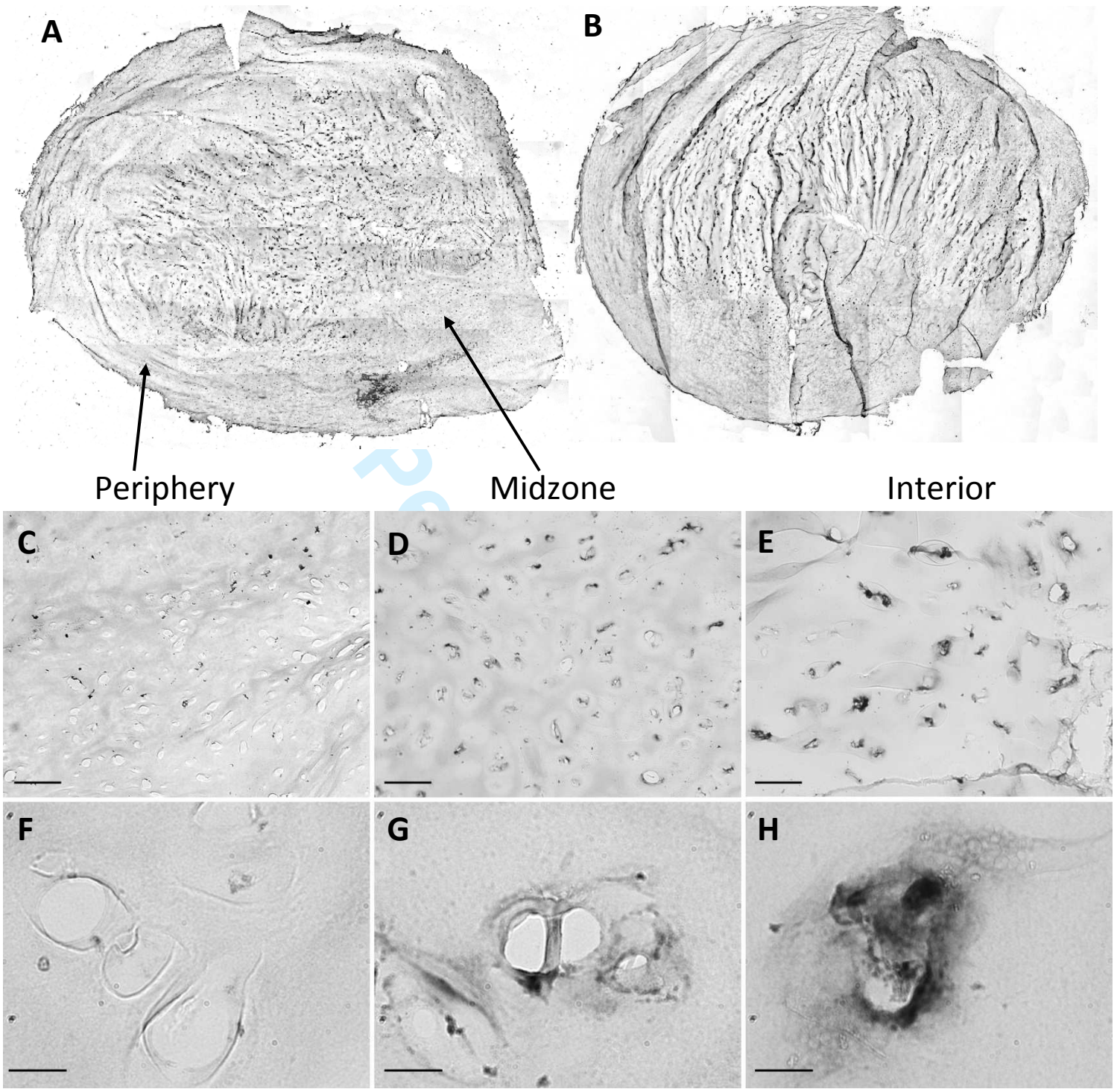
Control
PC3
A
B
Periphery
Midzone
Interior
C
D
E
F
G
H

Supplemental Figure. Electron probe microanalysis of 100 equally spaced points over a transverse section of costal cartilage. Sodium is present only in the central 48 points (boxed), and not at the peripheral points, which contain Sulfur only (circled).

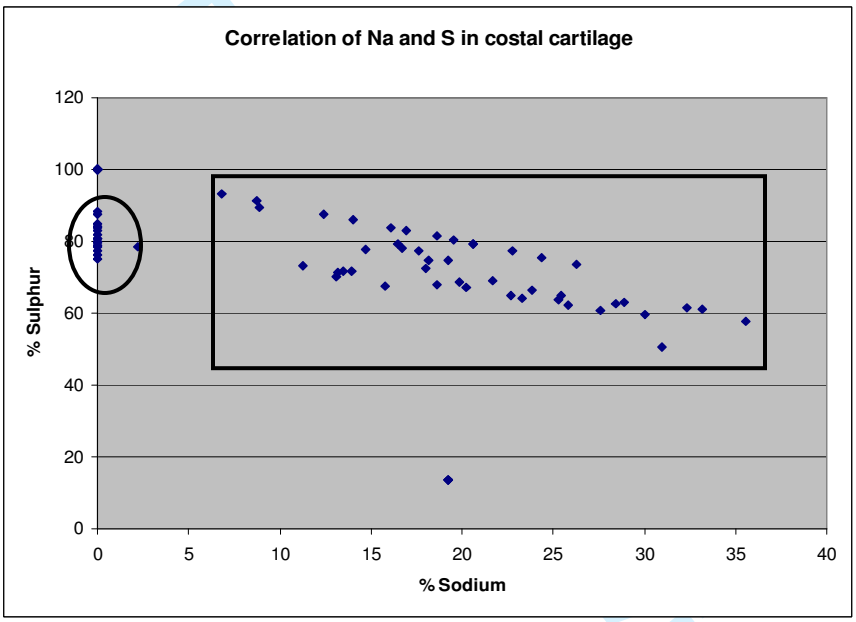

Decorin Expression, Straw-like Structure, and Differentiation of Human Costal Cartilage.

Stacey MW[1,2], Grubb J[1], Asmar A[1], Pryor J[1], El-Sayed Ali[3] H, Cao W[3], Beskok A[4], Dutta D[4], Darby DA[5], Fecteau A[6], Werner A[7], Kelly RE Jr[8].

[1]Frank Reidy Research Center for Bioelectrics, Old Dominion University, Norfolk, VA USA

[2] Department of Pediatrics, Eastern Virginia Medical School, Norfolk VA USA

[3] Applied Research Center, Electrical and Computer Engineering, Old Dominion University, Norfolk, VA

[4]Institute of Micro & Nanotechnology, Old Dominion University, Norfolk, VA

[5] Oceanography and Earth Sciences, Old Dominion University, Norfolk, VA

[6] Division of General Surgery, Hospital for Sick Children, Toronto, Canada.

[7] Dept of Pathology, Eastern Virginia Medical School and Med Director of Laboratories, Children's Hospital of The King's Daughters, Norfolk VA

[8] Department of Surgery, Eastern Virginia Medical School and Pediatric Surgery Division, Children's Hospital of the King's Daughters, Norfolk VA

Corresponding author:
Dr. Michael Stacey, Frank Reidy Research Center for Bioelectrics, 4211 Monarch Way, Suite 300, Norfolk, VA 23508 USA
Email: mstacey@odu.edu
Telephone: 757 683 2245
Fax: 757 451 1010

Running head Human costal cartilage

Key Words Pectus carinatum, chest wall deformities, connective tissue, SLRPs, AFM, gene ratio,

ABSTRACT

Costal cartilage is much understudied compared to the load bearing cartilages. Abnormally grown costal cartilages are associated with the inherited chest wall deformities pectus excavatum and pectus carinatum resulting in sunken or pigeon chest respectively. A lack of understanding of the ultrastructural and molecular biology of costal cartilage is a major confounder in predicting causes and outcomes of these disorders. The present study analyzed the structure of marginal human costal cartilage (ribs 6-10) through scanning electron and atomic force microscopy and identified the presence of straw-like structures running longitudinally. We also demonstrated that chondrocytes tend to occur singly or as doublets and that centrally located cells produce high levels of aggrecan compared to more peripherally located cells measured by immunohistochemistry. Gene expression from mRNA extracted from cartilage showed high levels of decorin expression, likely associated with the large, complex tubular structures running through this cartilage type. *COL2A1, ACAN* and *TIMP1* also showed higher levels of expression compared to *ACTB*. Analysis of gene expression ratios demonstrate that costal cartilage is under differentiated compared to published ratios for articular cartilage, likely due to the vastly different biomechanical environments of each cartilage type. Further studies need to establish whether findings described here from the costal margins are significantly different to cartilage of the 'true ribs' and how these values change with age.

INTRODUCTION

Costal cartilage, a type of hyaline cartilage, connects each of ribs 1-5 to the sternum and ribs 6-10, which are fused, to the sternum as the costal margin. They remain cartilaginous throughout life and provide both strength and flexibility to the chest wall. Disorders of the chest wall can cause significant disfigurement with associated cardiac, pulmonary, and psychological manifestations and are classified as sunken chest (pectus excavatum, PE) or pigeon chest (pectus carinatum, PC) [1]. The costal cartilages of these patients are described as abnormally grown and weak. Disorders of costal cartilage are common, affecting approximately 1/400-1/1,000 individuals, show complex inheritance patterns in families, and affect primarily males (M4:F1) [2, 3, 4, 5]. Chest wall deformities are phenotypically variable and surgical repair outcomes can be unpredictable. The basic molecular characteristics that define a healthy human costal cartilage are largely unknown, and a lack of understanding of the ultrastructural and molecular biology of costal cartilage is a major confounder in predicting outcomes and causes chest wall deformities.

Recent work [6] described a decrease in the biomechanical stability of costal cartilage in pectus excavatum patients and suggested a disorderly arrangement and distribution of collagen fibers. Other authors have suggested that atypical collagen fibers may be implicated in chest wall deformities [7, 8]. The arrangement of collagen fibers in costal cartilage has not been described in detail; however, highly ordered fiber formation was described [9] in the surrounding perichondrium. Growth of human costal cartilage chondrocytes *in vitro* shows high levels of *COL2A1* and *ACAN* expression and low levels of *COL1A1* at low culture passage, typical of a differentiated cell [10]. Differences in the variable number of tandem repeat units of chondroitin sulphate attachment sites were observed in *ACAN* with significantly more repeats (27) being present in patients with chest wall deformities [11].

TGFβ1 signaling plays a key role in cartilage growth and ECM turnover. Cells are extremely sensitive to levels of TGFβ1 and, therefore, regulation of this growth factor is important in normal growth and development. Genes activated via TGFβ pathways include *SOX9*, a major transcription factor of chondrocyte differentiation and regulator of

Deleted: Cartilage tissue consists of chondrocytes and extracellular matrix (ECM) that primarily comprises collagens, small and large proteoglycans and water.

Deleted: an

Deleted: factor

Deleted: cartilage

ACAN and *COL2A1* expression. In addition, *TIMP1,* a regulator of the matrix metalloproteinase's (MMP 8 and 13), is positively regulated by the TGFβ1 pathway [12].

Small leucine-rich proteoglycans (SLRPs) are small proteoglycans that are highly expressed in cartilage. Regulation of collagen fibrillogenesis is an important function shared by many SLRPs, and null mutations have been shown to lead to abnormal collagen architecture in mice [13]. Additionally, SLRPs mediate cell metabolism by binding to growth factors, including members of the superfamily TGFβ1 [14]. The causes of PE and PC are unknown; however, SLRPs can regulate ECM growth and fibrillogenesis by controlling TGFβ availability, suggesting a mechanistic role for SLRPs in these disorders. Biglycan deficiency has been shown to cause spontaneous aortic dissection and rupture in mice [15], and is also a characteristic of Marfan syndrome, a syndrome known to exhibit chest wall deformities. Decorin function is consistent with functions related to fibrillogenesis [16, 17]. A critical concept of SLRP function is compensation of one SLRP function over another. In the absence of biglycan, decorin is up-regulated and, therefore, differences in gene expression ratios may be apparent. Our central hypothesis is that abnormal expression of *BGN* and *DCN* will be observed in patients with chest wall deformities.

A thorough knowledge on the expression patterns of genes responsible for chondrogenesis in costal cartilage would provide insights into the role of these proteins in chest wall deformities and offer a biological rationale for the variability observed in outcome of surgery [18, 19, 20]. The objective of this study was to identify ultrastructural morphology and protein localization, investigate relative levels of expression of key genes required for chondrogenesis, and compare changes in normal costal cartilage and chest wall deformity.

MATERIALS AND METHODS

2.1 Subjects

Human costal cartilage was obtained from 4 patients with pectus carinatum severe enough to warrant surgical repair. Informed consent was obtained following IRB approval of the protocol at Eastern Virginia Medical School. The IRB protocol currently prevents disclosure of many clinical features, and thus close correlation of clinical

phenotype with expression is not possible. Costal cartilage samples were collected from ribs 6-8 at surgery. Experiments were performed on the round, rod-like, mid-sections of cartilage. All patients were male, with an age range of early teen to early 20's. Apparently normal costal cartilage was obtained from an age-matched-control, a 15 year old male and processed within 24 hours. All samples were snap frozen in liquid nitrogen and stored at -80°C until use.

Deleted: , cartilages that fuse and join ribs to the lower sternum as the costal margin

Deleted: described here

Deleted: from a recently deceased age-matched-control, a 15 year old male who died of unrelated causes

2.2 Ultrastructural analysis

Scanning electron microscopy (SEM) is a well-described technique employed for ultrastructural studies of cells and tissues. Cartilage, samples were cut into small sections approximately 3mm thick, washed three times in Sorenson's buffer and digested at 37°C for 48 hours in trypsin (1mg/ml) and hyaluronidase (1mg/ml) in Sorenson's buffer [21]. Samples were washed thoroughly in PBS and fixed in 2.5% glutaraldehyde in phosphate buffered saline for 2.5 hours. Samples were rinsed in deionized water, dehydrated through an ethanol series, dried and mounted on carbon discs, gold sputtered, and examined using a JSM-6060LV SEM (JEOL, Tokyo, Japan) operating at 5 keV to minimize sample damage. Images were captured electronically and fiber measurements made using Image J software.

Deleted: After surgical removal of costal c

Deleted:

Deleted: to eliminate charge build-up during SEM analysis

Deleted: the low voltage of

Deleted: any

2.3 Atomic Force Microscopy (AFM)

Collagen straws were released from small pieces of tissue by brief homogenization and digestion with 0.1mg/ml hyaluronidase and 0.1mg/ml trypsin in Sorenson's buffer. Samples were fixed in ice cold acetone and fiber diameters measured using a Nanonics Multiview-4000 multi-probe AFM.

2.4 Immunohistochemistry

Confirmation of aggrecan gene expression and protein distribution were made by immunohistochemistry. Frozen cartilage samples were mounted in CRYO-OCT Compound (Tissue-Tek, CA USA) and sections (5µm) generated using a Microm HM525 cryostat. Sections were fixed in ice-cold acetone. Blocking, incubation with primary and secondary antibodies and washing were performed following manufacturer's guidelines for each antibody. Tissues were incubated with a mouse monoclonal antibody specific for aggrecan (sc-73693, Santa Cruz, Santa Cruz, CA). The antibody was raised against recombinant aggrecan from human origin. Negative controls were produced using

Deleted: Gene expression c

Deleted: confirmed for aggrecan

Deleted: (Santa Cruz Biotechnology, CA USA)

normal mouse IgG included in the ImmunoCruz mouse LSAB staining system (sc-2050, Santa Cruz). Electronic images were captured using a CCD camera through an Olympus BX51 with Metamorph and Image J software for semi and quantitative analysis of protein deposition.

2.5 Chondrocyte distribution

Cartilage consists mainly of proteoglycans and collagens, with chondrocytes sparsely distributed throughout the matrix. We catalogued the distribution pattern of 586 and 999 chondrocytes in transverse sections of costal cartilage from PC3 and Con3 respectively, through an Olympus BX51 microscope, as groups of 1-4+ cells per cluster located interiorly or peripherally. Interior cells were within the strongly expressing aggrecan region, and peripheral cells outside.

2.6 Reverse Transcription and Real-Time PCR Analysis

Cartilage was removed from -80°C and transverse sections cut at approximately 3-5mm on dry ice and placed into RNALater (Qiagen, CA USA). Samples were quickly weighed and approximately 100mg of costal cartilage was ground to a powder with a liquid nitrogen immersed pestle and mortar. RNA was isolated and genomic DNA eliminated by completing RNA extraction using a RNeasy Plus Mini Kit and RT-First Strand Kit (Qiagen, CA USA). All polymerase chain reactions (PCR) were performed on a BioRad CFX96 system in 25µl reactions using SYBR green detection (Qiagen, CA USA). Gene expression by PCR was performed on genes described in Table 1, all compared to the housekeeping gene *ACTB*. All primers were from Qiagen, CA USA. The reaction conditions were identical for all primers, 95°C for 10 minutes, then 40 rounds of 95°C for 15 seconds and 60°C for 60 seconds. Reaction specificities were assessed with a melt curve of 65°C to 95°C in 0.2°C increments. All experiments were in triplicate and performed with positive and negative controls. At least two independent extractions were included from samples stored at 4°C in RNALater. Data were standardized to housekeeping *ACTB* values for all samples using the delta Ct method.

2.7 Statistical Analysis

Statistical analysis was performed using Student t-test to determine significance between sample and control means. For all tests, $p < 0.05$ indicated the difference as significant.

Deleted: Detection was through horseradish peroxidase/DAB reaction using the ImmunoCruz staining system (Santa Cruz Biotechnology, CA USA).

Deleted: 2

Deleted: of this

Deleted:

Deleted: and groups of 3 or more

Formatted: Superscript

Deleted: A

Deleted: Qiagen

Comment [mws1]: RNALater is a proprietary reagent stabilizes RNA and gave repeatable results within the time frame of our experiments. I can separate out the results, but I think this is more of a technical issue that may take away from the main thrust of the paper.

Formatted: Superscript

RESULTS

3.1. Electron Microscopy and AFM

Costal cartilage is a much understudied tissue type, both ultra structurally and genetically. We provide a first description of these properties in samples of human costal cartilage. Figures 1a and 1b are representative SEM images of a transverse cross-section of costal cartilage taken from a mid-section. Figure 1a shows a fracture in the cartilage, estimated as the inner-middle zone, exposing collagen fibers of approximately 600nm diameter. Fibers are assembled into extremely large complexes of many µm (arrowed) that run parallel to the length of the cartilage. Figure 1b is a higher magnification of the boxed area and shows that each fiber forms a nanostraw of approximately 650nm external diameter and 250nm internal lumen diameter. Images of longitudinal sections show a well-defined organization of collagen fibers approximately 20µm diameter and cellular lacunae (Figure 1c). We measured the diameters from 150 clearly defined fibers from SEM images (Table 2) and found that most were in the range from 0.1-100 µm. The smallest (<0.1µm) would most-likely represent the collagen fibrils, the midsize (~1µm) would represent the "microtubes" and the largest (~100µm) would be large fascicle-like structures. Cartilage homogenization and digestion released nanostraw fibers and allowed further characterization by AFM. Figure 1d shows an AFM image of branching/splitting fibers with a maximum diameter of approximately 740nm. Clearly, costal cartilage has large fiber dimensions with complex structures formed through finely tuned fibrillogenesis.

Deleted: t

Deleted: come

Deleted: together to form an

Deleted: with bundles

Deleted: of

Deleted: We measured diameters from 150 clearly defined fibers from SEM images and found measurements ranged from 43nm to 95.2µm. The distribution of diameter sizes is summarized in Table 1 and shows fibers are processed and packaged into thick fibrous structures.

Deleted: that are

3.2 Aggrecan immunohistochemistry

Aggrecan deposition from cells appeared to be a function of location. Figure 2 shows a representative cross-section of costal cartilage with cells located centrally exhibiting intense aggrecan staining (A) compared to the more peripherally located cells (B) and outer most cells (C). Interestingly, we were able to show increased levels of sodium ions in the same central region by electron probe microanalysis (EPMA, supplemental figure), showing that positively charged ions were drawn in to achieve electroneutrality.

3.3 Chondrocyte distribution

The organization of chondrocytes in cartilage is not considered to be random, and different cartilage types have different configurations of singles, pairs, clusters or strings

of cells. The percentage number of cell clusters observed in the interior was 1 cell (68.5% and 60.2%), 2 cells (23% and 27.3%), 3 cells (4.3% and 10.1%) and 4+ cells (4.2% and 2.4%) respectively for PC3 and Control. For peripherally located cells, observed clusters were 1 cell (86.9% and 73.0%), 2 cells (12.6% and 19.7%), 3 cells (0.5% and 5.5%) and 4+ cells (0% and 1.8%) respectively for PC3 and Control. There is a trend towards higher cell clusters in the interior; however, there appears to be no differences in cell distribution between PC3 and age-matched control. No strings were observed.

Deleted: We did not find any apparent

Deleted: We observed over 90% of cells as singles or doublets in control (90.1%) and PC3 (95.4%) and only 1.04% and 1.08%, respectively, as clusters of 4 or more cells

3.4 Gene expression

Due to the unusual structure of costal cartilage we undertook analysis of gene expression to determine presence of the main constituents of cartilage; collagen type II, and the large aggregating proteoglycan, aggrecan. We also examined other genes that play a role in growth, structure and differentiation of cartilage. *BGN, NYX, CACNA1F* and *TIMP1* were of interest because these genes are located on the human X-chromosome, where affected individuals are predominantly male and possess only a single X-chromosome [2, 3].

Deleted: and may be significant in development of chest wall deformities

Costal cartilage from individuals with chest wall deformities is described as abnormally grown and weak. Typically, surgical repair takes place during teenage years to early 20's. Phenotypically, there is considerable variation of the clinical condition of PC, reflecting the complex nature and inheritance observed in these families. Variation in gene expression between samples is, therefore, expected; however, it is unknown whether the expression of matrix genes will be affected by surgical procedures. We compared gene expression of 4 patients with pectus carinatum to an age-matched-control. Table 3 shows *COL2A1*, *DCN, ACAN,* and *TIMP1* are all highly expressed compared to *ACTB*. Sample variation was noted, although, as expected, *COL2A1* was expressed to the highest level in all samples.

Deleted: expected

Deleted: Significant changes in gene expression are indicative of potential genetic influences on phenotype.

Compared to control, PC1 showed significant reduction in expression of *DCN* ($p<0.001$) and *TIMP1* ($p<0.001$). PC3 showed significantly lower expression of *COL2A1* ($p<0.001$) and like PC4, both showed decreased expression of *ACAN* ($p<0.03$ and $p<0.024$, respectively). PC4 also showed significantly higher expression of *TIMP1* ($p<0.001$) and decreased expression of *BGN* ($p<0.04$). PC2 showed significant reduction in expression of *COL2A1* ($p<0.01$), *DCN* ($p<0.0002$), *TIMP1* ($p<0.001$), *BGN* ($p<0.03$)

and *FBN1* ($p<0.01$). This sample, like all PC samples, was immediately processed from the operating room, although results suggest possible degradation of this sample.

Many patients with chest wall deformities are considered Marfanoid-like [22] without fulfilling all criteria for diagnosis of Marfan syndrome, including mutations of the fibrillin-1 gene. The expression of this gene was not significantly different between control and patients, with the exception of PC2 ($p<0.01$). Expression of the X-linked genes *NYX* and *CACNA1F* was not detected in any samples. Overall, deregulation of *TIMP1* expression was evident in 3/4 PC samples, and expression of *DCN* was significantly lower in 2/4, suggestive of roles for fibrillogenesis and matrix turnover. The differentiation status of cartilage can be equated to the ratio of *COL2A1*, present in differentiated cartilage, to *COL1A1*, present at higher levels in more undifferentiated cartilage. We compared ratios of gene expression to published data. Ratios of the differentiation markers *COL2A1:ACAN* and *COL2A1:COL1A1* are low in PC patients and control (Table 4) compared to rabbit articular cartilage (1090 and 1790, respectively) but both are highly comparable to the nucleus pulposus region of lumbar discs (23 and 930 respectively), [23]. The ratios of *ACAN:COL1A1* fall between those reported for fully differentiated rat chondrosarcoma cells (78.4) and dedifferentiated chondrocytes cultured from costal cartilage (4.6) [24]. A high expression ratio of *COL2A1:COL1A1* (294.6) in human articular cartilage has been reported [25], but here results are referenced to *GAPDH* rather than *ACTB*. Overall, these results suggest costal cartilage is at an intermediate stage of differentiation and likely represents the different functional requirements of this tissue compared to articular cartilage. Small differences exist between patients and between patients and control (Table 4), suggesting that gene ratios measured here are not major contributors to chest wall abnormalities in these samples. Interestingly, *DCN* is expressed at high levels compared to *BGN*. As well as binding growth factors, both SLRPs have a role in fibrillogenesis and were hypothesized to play a role in the etiology of chest wall deformities. The high *DCN/BGN* ratio strongly suggests the importance of decorin expression in costal cartilage morphology. Decorin is present at high levels during tendon (fibro-cartilage) development and persists until thick fibers are formed [26], thus parallels with costal cartilage (hyaline cartilage) are apparent.

Deleted: To solidify this data, examination of further age-match controls and PC samples are required. ¶

DISCUSSION

Costal cartilage is a much understudied cartilage where deformities have significant clinical consequences. A lack of understanding of molecular and ultrastructural properties hampers understanding events leading to these disorders. The present study compared relative gene expression of major genes of chondrogenesis from patients with pectus carinatum to an age-matched-control to answer questions relating to maintenance and differentiation. Perhaps the most important observations are 1) the longitudinal straw-like arrangement of collagen fibers, 2) the centrally located deposition of aggrecan, 3) the high level of decorin expression, and 4) gene ratios indicating under differentiation compared to articular cartilage.

The ultrastructural electron microscopy images show that human costal cartilage is unlike other cartilage types. Images appear to show that individual fibers are assembled to collectively form very thick, fascicle structures appearing to consist of large numbers of collagen nanostraws that run parallel along the cartilage length. A similar observation of collagen tubules in juvenile rabbit tibia articular cartilage was reported [27], but this is the first report in human costal cartilage. The cartilage template of long bones is similar to costal cartilage in that they are both long, thick, rod-like structures and, therefore, although functionally different, ultrastructural similarities may be expected in response to cell maintenance and collagen fiber deposition under these conditions.

The morphological form of costal cartilage and how this relates to function is currently unknown. The presence of straw-like structures may provide strength and a means of gas and nutrient exchange to cells by fluid flow whose movement is dependent upon cartilage movement during breathing. Costal cartilage can be nearly 1cm diameter, outside of the range of diffusion to maintain centrally located cells [28]. Hypoxia or low pH has been shown to act as a trigger for aggrecan and collagen type II production through induction of hypoxia inducible factor 1-α and *SOX9*, as well as inhibit *COL1A1* expression [29, 30]. Similarities with inter vertebral discs are noteworthy. Cells embedded within the centrally located nucleosus pulposus experience hypoxia and express aggrecan under the regulation of the hypoxia induced P13K/AKT signaling pathways via modulation of *SOX9* [31]. It appears that as cells become centrally located

Deleted: come together

Deleted: . These structures

Deleted: a

Deleted: Interestingly, centrally located cells produce high levels of aggrecan.

Deleted: ,

they experience hypoxia and lower pH. *ACAN* expression is induced with cationic uptake that we confirmed by Electron Probe Micro Analysis.

Few studies have been undertaken on chondrocyte distribution within cartilage, yet cell density and arrangements are considered to be critical to function. Cellular clusters [32], pairs [33], and rows [34], have been reported. A more extensive study [35] in the superficial zone of articular cartilage identified complex patterns that appear to be location specific. A spatial relationship between collagen fiber alignment and cellular organization was suggested [34], with chondrocytes running parallel to adjacent fibers. Longitudinally, we also note the presence of lacunae between the large fibrous structures. The predominance of single and doublets in costal cartilage suggests cells undergo relatively few divisions. The absence of extensive strings and clusters is likely due to the different biomechanical forces experienced by costal cartilage compared to cartilage covering ball and socket joints.

SLRPs play an important role in fibrillogenesis and shape the architecture and mechanical properties of the collagen matrix. SLRP-deficient animals exhibit a wide array of diseases, mostly resulting from abnormal fibrillogenesis [13]. We examined the expression of three SLRPs; *DCN* and the X-linked genes *BGN* and *NYX*. *NYX* expression was not detected in any samples of costal cartilage and likely does not play a role in chondrogenesis. *DCN* has a role in modulating cartilage fibril growth, thickness, and orientation. Indeed, *DCN* deficiency introduces tissue-specific variations in range, mean, and distribution of collagen fibril diameters compared to wild-type. Interestingly, *DCN* deficiency also leads to random orientation of collagen fibrils in periodontal ligament instead of the usual parallel orientation [36]. Regional variation in localization of proteoglycans decorin, biglycan, and aggrecan has been reported in tendon, with decorin highest in regions of greatest tensile strength [37]. However, tensile strength of costal cartilage appears to reduce as it matures from childhood to teenage/early twenties years [38], suggesting rearrangement of collagen fibers with age that may be proteoglycan mediated. The highly aligned collagen fibers observed in costal cartilage show similarities to the aligned fibers of tendon. The hierarchical assembly of collagen fibers in tendon is a multistep process leading to the mature tissue [39]. Briefly, collagen fibril intermediates are assembled and undergo linear and lateral growth. Intercalation of fibrils

Deleted: in costal cartilage,
Deleted: and
Deleted: 1
Deleted: 2
Deleted: 3
Deleted: 4
Deleted: 3
Deleted: regulate the availability of growth factors and, taken together,
Deleted: 5
Deleted: 6
Deleted: 7

is necessary for growth resulting in mature fibers and fibrils necessary for mechanical integrity. The interactions with fibril associated collagens and SLRPs have been implicated in the form and function of mature tendon. In costal cartilage an additional layer of complexity in the formation of tubules is intriguing, and suggests, by the high level of *DCN* expression, that decorin is crucial in this morphology.

The relative expression of genes expressed as a ratio has been used to determine differentiation status of cartilage where *COL2A1* and *ACAN* are highly expressed compared to *COL1A1*. This ratio decreases rapidly as chondrocytes dedifferentiate *in vitro*. Adaption of tissue to its mechanical constraints leads to different qualitative compositions. Costal cartilage exhibits a phenotype consistent with cartilage, with high *COL2A1/COL1A1, COL2A1/ACAN* and *ACAN/COL1A1*ratios, although *COL2A1/ACAN* and *COL2A1/COL1A1*ratios were considerably lower than rabbit articular cartilage also normalized to *ACTB* [24] suggesting *COL2A1* expression may be reduced. Expression levels in costal cartilage are closer to those reported in the nucleus pulposus of lumbar discs than to articular cartilage. Both nucleus pulposus and costal cartilage expression levels likely represent the functional requirements of their respective mechanical loads that are considerably different to that experienced in articular cartilage.

The present study has uncovered a new dimension of complexity that has not previously been reported. The study here describes findings that are generated from samples of costal cartilage that are generally removed at surgery, ribs 6-8. Although the current study has relatively few samples we feel that the overall results indicate that there are several important features unique to costal cartilage. Future work will examine variations along and between different ribs to more closely correlate variations of functions that may occur within the environment of the chest wall. Connective tissue gene arrays will allow analysis of many more genes simultaneously correlated to clinical picture. The etiology of chest wall deformity is complex. Changed growth characteristics of costal cartilage in patients may be a secondary characteristic due to external factors. Alternatively deformed cartilage may be intrinsic due to the inherited, albeit complex, nature of these disorders. Future work will aim to clarify these discrepancies.

Deleted: The formation and orientation of straw-like structures observed in costal cartilage

Deleted: Alternatively, there is a possibility that *DCN* is being over expressed as a means of compensation for reduced expression of *BGN*.

Deleted: is

Deleted: are grown

Deleted: where *COL1A1* expression increases and *COL2A1* and *ACAN* expression decrease during dedifferentiation

Acknowledgments

We thank Dr M. Young, National Institute of Dental and Craniofacial Research, NIH and Dr C. Osgood, College of Sciences, Old Dominion University for critical review of this manuscript, and Old Dominion University Office of Research for seed funding grant.

Declaration of interest: The authors have declared no conflict of interest.

References

[1] Kelly RE, Shamberger RC, Mellins RB, Mitchell KK, Lawson ML, Oldham K, Azizkhan RG, Hebra AV, Nuss D, Goretsky MJ, Sharp RJ, Holcomb GW, Shim WKT, Megison SM, Moss RL, Fecteau AH, Colombani PM, Bagley TC and Moskowitz AB. Prospective Multicenter Study of Surgical Correction of Pectus Excavatum: Design, Perioperative Complications, Pain, and Baseline Pulmonary Function Facilitated by Internet-Based Data Collection. J.Am. College of Surgeons. (2007) 205: 205-216

[2] Horth L, Stacey MW, Benjamin T, Segna K, Proud VK, Nuss D, Kelly RE. Genetic analysis of inheritance of *Pectus excavatum.* J. Pediatric Genetics. (2012) In press

[3] Creswick H, Stacey M, Kelly R, Burke B, Gustin T, Mitchell K, Nuss D, Harvey H, Croitoru D, Goretsky M, Vasser E, Fox P, Goldblatt S, Tabangin M, Proud V. Family studies on the inheritance of pectus excavatum. J. Pediatr. Surg. (2006) 41:1699-1703

[4] Leung AK, Hoo JJ. Familial congenital funnel chest. Am. J. Med. Genet. (1987). 26: 887-890

[5] Sugiura, Y. A family with funnel chest in three generations. Jpn. J. Hum. Genet. (1977). 22: 287-289.

[6] Feng J, Hu T, Liu W, Zhang S, Tang Y, Chen R, Jiang X, Wei F. The biomechanical, morphologic, and histochemical properties of the costal cartilages in children with pectus excavatum. J. Pediat. Surg. (2001). 36: 1770-1776.

[7] Rupprecht H, Hümmer, HP. Stöß, H. Waldherr T. Pathogenesis of the Chest Wall Deformities - Electron Microscope Studies and Analysis of Trace Elements in the Cartilage of the Ribs. Eur J Pediatr Surg (1987). 42(4): 228-229

[8] Fokin AA, Nury M. Steuerwald M, Ahrens William A, Allen KE. Anatomical, Histologic, and Genetic Characteristics of Congenital Chest Wall Deformities. Semin Thorac Cardiovasc Surg. (2009). 21(1):44-57

[9] Forman JL, del Pozo de Dios E, Dalmases CA, Kent RW. The contribution of the perichondrium to the structural mechanical behavior of the costal-cartilage. J. Biomech. Eng. (2010) 132; /094501 doi: 10.1115/1.4001976

[10] Zhang Y, Chai G, Liu W, Cui L,Cao YL. Age-related changes in growth and metabolism function of human costal chondrocytes cultured in vitro. Zhonghua Zheng Xing Wai Ke Zhi (2004) 20; 372-376

[11] Stacey M, Neumann S, Dooley A, Segna K, Kelly R, Nuss D, Kuhn A, Goretsky M, Fecteau A, Pastor A, Proud V. Variable Number of Tandem Repeat Polymorphisms (VNTRs) in the *ACAN* Gene Associated with Pectus Excavatum. Clin. Genet. (2010). 78;502-504

[12] El Mabrouk M, Qureshi HY, Li QW, Sylvester J, Zafarullah M. Interleukin-4 antagonizes oncostatin M and transforming growth factor beta-induced responses in articular cartilage. J. Cell. Biochem. (2008).103: 588-597.

[13] Ameye L, Young MF. Mice deficient in small leucine-rich proteoglycans: novel in vivo models for osteoporosis, osteoarthritis, Ehlers-Danlos syndrome, muscular dystrophy, and corneal diseases. Glycobiology (2002).12: 107R-116R.

[14] Hildebrand A, Romaris M, Ramussen LM, Heingard D, Twardzik DR, Border WA, Ruoslahti E Interaction of the small interstitial proteoglycans biglycan, decorin and fibromodulin with transforming growth factor β. Biochem. J. (1994). 302: 527-534

[15] Heegaard AM, Corsi A, Danielsen CC, Nielsen KL, Jorgensen HL, Riminucci M, Young MF, Bianco P. Biglycan Deficiency Causes Spontaneous Aortic Dissection and Rupture in Mice. Circulation. (2007);115:2731-2738.

[16] Bianco P, Fisher LW, Young MF, Termine JD, Robey PG. Expression and localization of the two small proteoglycans biglycan and decorin in developing human skeletal and non-skeletal tissues. J. Histochem. Cytochem. (1990). 38: 1549-1563

[17] Kalamajski S, Oldberg A. The role of small leucine-rich proteoglycans in collagen fibrillogenesis. Matrix Biol. (2010) 29; 248-253

[18] Antonoff MB, Saltzman DA, Hess DJ, Acton RD. Retrospective review of reoperative pectus excavatum repairs. J. Pediatr Surg. (2010). 45(1):200-5.

[19] Bouchard S, Hong AR, Gilchrist BF, Kuenzler KA. Catastrophic cardiac injuries encountered during the minimally invasive repair of pectus excavatum. Semin. Pediatr. Surg. (2009) 18(2):66-72.

[20] Swanson JW, Colombani PM. Reactive pectus carinatum in patients treated for pectus excavatum. J. Pediatr. Surg. (2008). 43(8):1468-73.

[21] Stolz M, Gottardi R, Raiteri R, Miot S, Martin I, Imer R, Staufer U, Raducanu A, Düggelin M, Baschong W, Daniels AU, Friederich NF, Aszodi A & Aebi U. Early detection of aging cartilage and osteoarthritis in mice and patient samples using atomic force microscopy. Nature Nanotechnology (2009) 4; 186-192

[22] Redlinger RE Jr., Rushing GD, Moskowitz AD, Kelly RE, Jr., Nuss D, Kuhn A, Obermeyer RJ, Goretsky MJ. Minimally invasive repair of pectus excavatum in patients with Marfan Syndrome and Marfanoid features. J. Pediatr. Surg. (2010). 45(1): 193-199

[23] Clouet J, Grimandi G, Pot-Vaucel M, Masson M, Fellah HB, Guigand L, Cherel Y, Bord E, Rannou F,Weiss P, Guicheux J and Vinatier C. (2009). Identification of phenotypic discriminating markers for intervertebral disc cells and articular chondrocytes. Rheumatology (2009) 48 (11): 1447-1450.

Deleted: ¶

Formatted: Space Before: 0 pt, After: 0 pt, Line spacing: single

Deleted: Goldring MB, Goldring SR. Osteoarthritis. J. Cell. Physiol. (2007). 213; 626-634¶
¶

[24] McAlinden A, Havlioglu N, Liang L, Davies SR, Sandell LJ. Alternative Splicing of Type II Procollagen Exon 2 Is Regulated by the Combination of a Weak 5′ Splice Site and an Adjacent Intronic Stem-loop Cis Element. J. Biol. Chem. (2005). 280; 32700-32711

[25] Martin I, Jakob M, Schafer D, Dick W, Spagnoli G, Heberer M. Quantitative analysis of gene expression in human articular cartilage from normal and osteoarthritic joints. Osteoarthr. Cartilage (2001) 9; 112-118

[26] Kalamajski S, Oldberg A. The role of small leucine-rich proteoglycans in collagen fibrillogenesis. Matrix Biology (2010) 29; 248-253

[27] Gwynn AP, Wade S, Kääb MJ, Owen GR, Richards RG. Freeze-substitution of rabbit tibial articular cartilage reveals that radial zone collagen fibers are tubules. J. Microsc. (2000) 197; 159-172

[28] Gibson JS, Milner PI, White R, Fairfax TP, Wilkins RJ. Oxygen and reactive oxygen species in articular cartilage: modulators of ionic homeostasis. Pflugers Arch. (2008) 455; 563-573

[29] Duval E, Leclercq S, Elissalde JM, Demoor M, Galera P, Boumediene K. Hypoxia-inducible factor 1α inhibits the fibroblast-like markers type I and type III collagen during hypoxia-induced chondrocyte redifferentiation. Arthritis Rheum. (2009) 60; 3038-3048

[30] Das RHJ, van Osch GJVM, Kreukniet M, Oostra J, Weinans H, Jahr H Effects of individual control of pH and hypoxia in chondrocyte culture. J. Orthop. Res. (2010). 28; 537-545

[31] Chin-Chang Cheng, Yoshiyasu Uchiyama, Akihiko Hiyama, Sachin Gajghate, Irving M. Shapiro, and Makarand V. Risbud. PI3K/AKT Regulates Aggrecan Gene Expression by Modulating Sox9 Expression and Activity in Nucleus Pulposus Cells of the Intervertebral Disc. J. Cell Physiol (2009) 221; 668-676

[32] Schumacher BL, Su JL, Lindley KM, Kuettner KE, Cole AA. Horizontally oriented clusters of multiple chondrons in the superficial zone of ankle, but not knee articular cartilage. Anat. Rec. (2002). 266; 241-248

[33] Jadin KD, Wong BL, Bae WC, Li KW, Williamson AK, Schumacher BL, Price JH, Sah RL. Depth-varying density and organization of chondrocytes in immature and mature bovine articular cartilage assessed by 3d imaging and analysis. J. Histochem. Cytochem. (2005). 53; 1109-1119

[34] Clark JM, Rudd E. Cell patterns in the surface of rabbit articular cartilage revealed by the backscatter mode of scanning electron microscopy. J. Orthop. Res. (1991). 9; 275-283

Formatted: Normal
Formatted: Line spacing: single
Formatted: Normal
Deleted: ¶
Deleted: 1
Deleted: 2
Deleted: 3

[35] Rolauffs B, Williams JM, Grodinsky AJ, Kuettner KE, Cole AA. Distinct horizontal patterns in the spatial organization of superficial zone chondrocytes of human joints. J. Struct. Biol. (2008). 162; 335-344

[36] Hakkinen L, Strassburger S, Kahari VM, Scott PG, Eichstetter I, Lozzo RV, Larjava H. A role for decorin in the structural organization of periodontal ligament. Lab. Invest. (2000) 80; 1869-1880

[37] Matuszewski PE, Chen YL, Szczesny SE, Lake S, Elliot DM, Soslowsky LJ, Dodge GR. Regional variation in human supraspinatus tendon proteoglycans: decorin, biglycan, and aggrecan. Connect. Tissue Res. (2012). Jan 6 Epub ahead of print.

[38] Yang Qing-Hua, Song Yu-Peng, Jiang Haiyue, Zhuang Hong-Xing. The significance of the biomechanical properties of costal cartilage in the timing of ear reconstruction surgery. J. of Plastic, Reconstructive and Aesthetic surgery (2011). 64; 742-746

[39] Zhang G, Young BB, Ezura Y, Favata M, Soslowsky, Chakravarti S, Birk DE. Development of tendon structure and function: Regulation of collagen fibrillogenesis J. Musculoskelet Neuronal Interact. (2005) 5; 5-21

Deleted: 4

Deleted: 5

Deleted: 6

Deleted: 7

Deleted: ¶
¶

Formatted: Line spacing: single

Deleted: Chin-Chang Cheng, Yoshiyasu Uchiyama, Akihiko Hiyama, Sachin Gajghate, Irving M. Shapiro, and Makarand V. Risbud. PI3K/AKT Regulates Aggrecan Gene Expression by Modulating Sox9 Expression and Activity in Nucleus Pulposus Cells of the Intervertebral Disc. J. Cell Physiol (2009) 221; 668-676¶
Stolz M, Gottardi R, Raiteri R, Miot S, Martin I, Imer R, Staufer U, Raducanu A, Düggelin M, Baschong W, Daniels AU, Friederich NF, Aszodi A & Aebi U. Early detection of aging cartilage and osteoarthritis in mice and patient samples using atomic force microscopy. Nature Nanotechnology (2009) 4; 186-192¶